



Counter-current operation of structured catalytically packed distillation columns: pressure drop, holdup and mixing

J. Ellenberger and R. Krishna

Department of Chemical Engineering, University of Amsterdam, Nieuwe Achtergracht 166,
1018 WV Amsterdam, The Netherlands

(Correspondence to R. Krishna, fax +31 20 5255604; Email: krishna@chemeng.chem.uva.nl)

Abstract - Structured packed columns, in which the catalyst particles are enclosed within wire gauze envelopes ("sandwiches") are promising reactor configurations for reactive distillation and hydroconversions. By allowing preferential channels for the gas and liquid phases, counter-current operation is achieved even for millimeter sized catalyst particles without the problem of flooding. This paper reports the results of a comprehensive experimental study of the hydrodynamics of structured packed columns of 0.1 and 0.24 m diameter. The pressure drop is found to increase sharply when the superficial liquid velocity exceeds a certain threshold value. This threshold corresponds to the situation in which a maximum flow of liquid in the packed channels is realized and the excess liquid flows through the "open" channels. The liquid flow in the open channel causes a sharp rise in the pressure drop. A model is developed to describe the holdup of liquid in the open channels. With increasing liquid flow rate, the pressure drop is found to increase exponentially with the liquid holdup within the open channels. Liquid phase residence time distribution studies lead to the conclusion that there is a good exchange of the liquid phase inside and outside the packed channels. The residence time distribution can be described by an axial dispersion model. Compared with a trickle bed reactor, the results of this study show that a structured packed column has a much larger operating window at a much lower pressure drop. © 1999 Elsevier Science Ltd. All rights reserved.

Keywords: structured packing; reactive distillation; counter-current operation; pressure drop; liquid holdup, liquid phase backmixing;

INTRODUCTION

There is considerable academic and industrial interest in the area of reactive (catalytic) distillation. The catalyst particle sizes used in such operations are usually in the 1 - 3 mm range. Counter-current operation in fixed beds packed with such particles is difficult because of flooding limitations. To overcome the limitations of flooding the catalyst particles have to be enveloped in wire gauze packing. The gas phase will flow preferentially in the open channels between the wire gauze envelopes. Xu *et al.* (1997) have studied the hydrodynamics of a column consisting of cylindrical catalyst "bundles". Bart and Landschützer (1996) have used the KATAPAK-S configuration of Sulzer for carrying out the process for making propyl acetate by reactive distillation. THE KATAPAK-S structure is shown in Figures 1 (a) schematically. There are several anticipated advantages of the KATAPAK-S configuration over the cylindrical bundles used by Xu *et al.* (1997). Firstly, there is no possibility of gas channeling in the KATAPAK-S configuration. Secondly, the catalyst envelopes in the KATAPAK-S structure consist of wire gauze structures, which are corrugated, and these corrugations cross each other at 90° angles. The effect of this is to ensure that the liquid

flowing inside the catalyst envelopes or "sandwiches" are forced to change directions frequently, ensuring good radial distribution. Computational fluid dynamics studies of such structures have confirmed that the radial distribution is significantly higher than in conventional trickle bed operations (Van Gulijk, 1998).

In the literature there is practically no information on the hydrodynamics and mixing characteristics of the intersecting sandwich structures shown in Fig. 1 (a). The purpose of the current study is to develop the necessary design information that could be used for design and scale up purposes.

EXPERIMENTAL

The experiments have been performed with two types of structured packing elements of similar geometry but different hydraulic diameters of the open channels of 7 and 20 mm respectively. These two packing configurations are housed in columns of 0.1 and 0.24 m diameters, see Figs 1 (b) and (c). Geometric details of the two configurations are listed in Table 1. Counter-current operation with the system air-water was studied. The "catalyst" particles used inside the sandwiches consisted of 1 mm glass spheres.

TABLE 1. CHARACTERISTIC PARAMETERS OF THE 0.10M AND 0.24M DIAMETER CATALYTICALLY STRUCTURED PACKED COLUMNS

| | $D_T = 0.1$ m | $D_T = 0.24$ m |
|--|------------------------|-------------------------|
| Number of packed sections used in the column | 9 | 6 |
| height L of the reactor, m | 1.8 | 1.705 |
| total mass of solids in reactor, kg | 9.1687 | 44.020 |
| solids holdup (including wire gauze) in reactor | 0.2047 | 0.1982 |
| Void fraction in reactor | 0.7953 | 0.8018 |
| Void fraction within "packed channels" | 0.454 | 0.505 |
| Volume fraction of "packed channels" in reactor, ϵ_{PC} | 0.375 | 0.400 |
| Volume fraction of "open" channels, ϵ_{OC} | 0.625 | 0.600 |
| rest volume V_{st} of water in reactor after an efflux time of half an hour, m^3 | 0.399×10^{-3} | 1.2425×10^{-3} |
| static liquid holdup in reactor | 0.0282 | 0.0161 |
| specific surface A_{sp} for the gas flow assuming the space between the glass spheres is completely filled with liquid, m^{-1} | 354.4 | 122.3 |
| hydraulic diameter of the open channels d_h , mm | 7 | 20 |
| Inclination of the corrugated sheets, α | 45° | 45° |

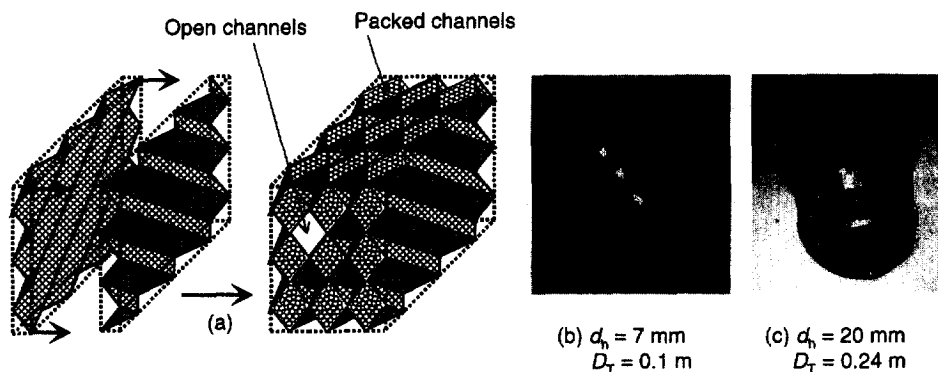


Figure 1. Schematic of structured packing with catalyst particles inside envelopes or "sandwiches". (b) and (c) Photograph of one section each of structured packing elements for the 0.1 and 0.24 m diameter columns.

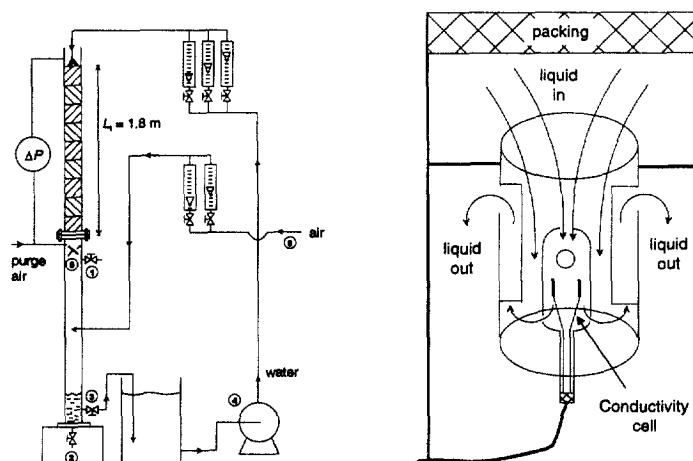


Figure 2. Schematic diagram of the experimental set-up. 1: valve for gas outlet; 2: valve for liquid drainage; 3: valve for liquid outlet control; 4: liquid pump; 5: quick shut-off valve; 6: air supply. The right diagram shows the layout of the thermal conductivity cell installed at the bottom of the packed section for measurement of the liquid phase residence time distribution.

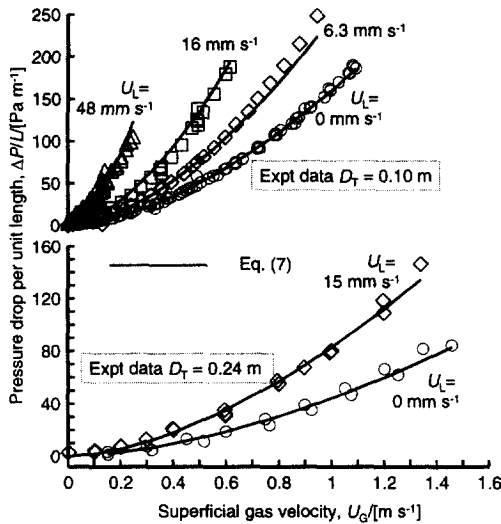


Figure 3. Increase in pressure drop with superficial gas and liquid velocities. Comparison of experiments with model for pressure drop.

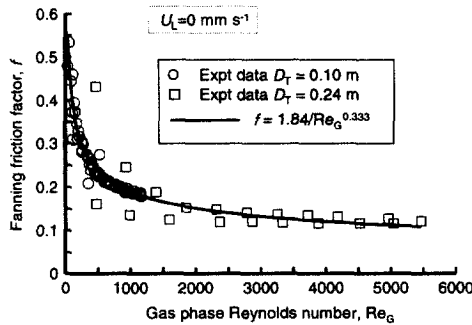


Figure 4. Fanning friction factor correlation for the two geometries.

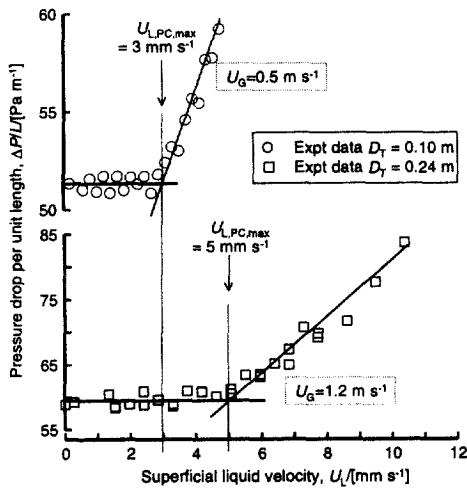


Figure 5. Maximum superficial liquid velocity $U_{L,PC,max}$ at which the pressure drop starts to increase for the 0.1 and 0.24 m diameter columns.

In Figure 2 a schematic view of the experimental set-up of the counter-current gas-liquid reactor ($D_T = 0.10$ m) with structured packing is shown. The liquid phase is pumped from a temperature-controlled reservoir to the top of the column by means of a centrifugal pump (Allweiler Italia, Type NB40 160 155). The recirculated liquid flow is controlled by one of the three carefully calibrated rotameters of different ranges. The maximum superficial liquid velocity is restricted to $U_L = 0.05$ m/s for the reactor with $D_T = 0.1$ m and $U_L = 0.02$ m/s for the reactor with $D_T = 0.24$ m.

Using another set of two calibrated rotameters of different ranges, a known gas flow can be fed to the bottom of the column. The gas leaves at the top of the column at atmospheric condition. A pressure sensor (Validyne) is used for the measurement of the pressure drop over the packed columns. The total height of the column is 4 m, the upper part of which is packed with the packing elements. The temperature of the liquid reservoir is maintained constant (equal to the gas temperature) by a large copper cooling tube connected to a Haake F3 temperature control unit.

When steady-state conditions have been established, the dynamic liquid holdup is measured by stopping the gas and liquid supply and closing the quick shut-off valve (5) simultaneously. Then the liquid in the bottom section of the column is removed. By opening the valves (5) and (2), the liquid in the upper part of the reactor is collected during half an hour. From the collected liquid mass, the dynamic liquid holdup can be calculated.

Measurements of the liquid phase residence-time-distribution (RTD) have been performed by injecting a tracer pulse (saturated NaCl-solution) at the top of the reactor and registration of the salt concentration as function of time at the bottom of the reactor. The tracer injection system as well as the conductivity cell for the tracer response measurements is positioned at the centerline of the reactor. A schematic view of the conductivity cell is shown at the right of Figure 2. Further details of our experimental set up and measurement techniques are available on our web site: <http://ct-cr4.chem.uva.nl/strucexpts>.

PRESSURE DROP AND LIQUID HOLDUP

The gas phase pressure drop per unit length of packing increases both with increasing superficial gas and liquid velocities, as seen from a selection of the experimental data presented in Fig. 3. The pressure drop experienced by the gas consists of two parts (1) the “dry” pressure drop and (2) the extra contribution due to the interaction between the gas and liquid phases. Assuming that the major portion of the gas flows through the “open channels” we may expect the dry pressure drop to be given by

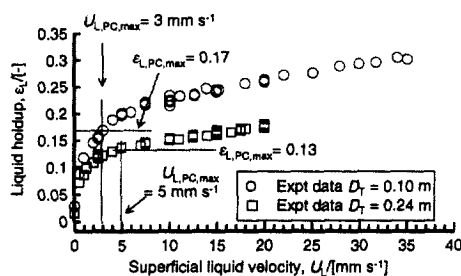


Figure 6. Liquid holdup as a function of the superficial liquid velocity. Also indicated in the figures are the superficial liquid velocities, and the corresponding liquid holdups, at which the pressure drop increases sharply (cf. Fig. 5).

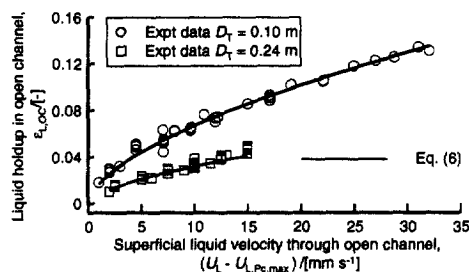


Figure 7. Liquid holdup in the open channel as a function of the superficial liquid velocity through the open channels.

$$\frac{\Delta P_{\text{dry}}}{L} = f \frac{1}{d_h} \rho_G v_G^2 \quad (1)$$

where f is the Fanning friction factor and d_h is the hydraulic diameter of the “open channels”, defined by

$$d_h = 4\epsilon_{OC}/A_{sp} \quad (2)$$

The gas velocity v_G through the “open channels” can be calculated from the superficial gas velocity U_G , the gas holdup in the “open channels” and the inclination of the corrugated sheets α .

$$v_G = U_G / (\epsilon_{OC} \sin \alpha) \quad (3)$$

Experimental data on the dry pressure drop leads to the following correlation for f as function of the gas phase Reynolds number Re_G as shown in Fig. 4

$$f = 1.84 / Re_G^{0.333} = 1.84 \left(\frac{\rho_G v_G d_h}{\eta_G} \right)^{-0.333} \quad (4)$$

Equation (4) holds equally well for describing the dry pressure drop in a Sulzer BX packed column (Cho *et al.*, 1995), emphasising the general applicability of our model. When the packing is irrigated, the liquid will flow through the “packed channels” until a maximum liquid holdup of the “packed channels” $\epsilon_{L,PC,max}$ is reached at the maximum superficial liquid velocity through the “packed channels” $U_{L,PC,max}$; see Fig. 5. In this range of irrigation, $U_L < U_{L,PC,max}$, the pressure drop will be equal to the dry pressure drop of the structured

packing. Further increase of the liquid flow will form a liquid film, flowing through the “open channels” resulting in a decrease of the hydraulic diameter of the “open channels”, a change in the specific surface A_{sp} , a change in the “roughness factor” of the surface, and an increase in the pressure drop. The decrease in the hydraulic diameter d_h is only a function of the liquid holdup in the “open channels” $\epsilon_{L,OC}$. The “roughness” of the liquid film in the “open channels” will decrease with decreasing film thickness and increasing viscosity and should be a function of $(Re_{L,OC}/Fr_{L,OC})$ where these dimensionless numbers are defined in terms of the liquid velocity through the open channels:

$$Fr_{L,OC} \equiv \frac{v_{L,OC}}{\sqrt{g d_h}}; \quad Re_{L,OC} \equiv \frac{v_{L,OC} \rho_L d_h}{\eta_L} \quad (5)$$

$$v_{L,OC} \equiv \frac{U_{L,OC}}{\epsilon_{OC} \sin \alpha} = \frac{U_L - U_{L,PC,max}}{\epsilon_{OC} \sin \alpha}$$

Corresponding to the values of $U_{L,PC,max}$, the maximum holdup of liquid in the packed channels, $\epsilon_{L,PC,max}$, can be determined from the experimental data for the two column diameters; see Fig. 6. The values of $\epsilon_{L,PC,max}$ are found to be 0.17 and 0.13 for the 0.1 and 0.24 m diameter columns. The liquid holdups in the open channels, determined from $\epsilon_{L,OC} = \epsilon_L - \epsilon_{L,PC,max}$, can be expected to correlate with $Re_{L,OC}$ and $Fr_{L,OC}$ as we expect surface tension forces to be unimportant in determining $\epsilon_{L,OC}$. Our experimental data lead to the following relation (cf. Fig. 7)

$$\epsilon_{L,OC} = 2.8 (Fr_{L,OC}^3 / Re_{L,OC})^{0.3} \quad (6)$$

The increase in pressure drop due to liquid flow in the open channel will also be affected by the “roughness” or “waviness” of the liquid films flowing in the open channels. Anticipating that roughness depends on the ratio $(Re_{L,OC}/Fr_{L,OC})$ we obtain a good correlation for the “wet” pressure drop as

$$\frac{\Delta P}{L} = \frac{\Delta P_{\text{dry}}}{L} \exp \left[1.3 \epsilon_{L,OC} \left(\frac{Re_{L,OC}}{Fr_{L,OC}} \right)^{0.3} \right] \quad (7)$$

Equation (7) describes the pressure drop per unit packing length within an average deviation of 20% for the range of gas and liquid velocities; see also Fig. 3. Equation (7) is also capable of describing the pressure drop in the Sulzer BX column (Cho *et al.*, 1995) and for a column filled with cylindrical “bales” of catalyst (Xu *et al.*, 1997).

LIQUID PHASE RTD

By injecting salt tracer in the inflowing liquid phase and monitoring the concentration at the bottom of the column the liquid phase residence time distributions were determined at various superficial liquid velocities U_L and at three different superficial gas velocities U_G . There was no significant influence of the superficial gas velocity on the residence time distribution. Typical RTD curves for $U_G = 0.3$ m/s and for various values of

U_L for the two columns are shown in Fig. 8. The measured liquid phase RTD is the same irrespective of whether the tracer is injected in the packed channels or in the open channels. This can be evidenced by the RTD measurements shown in Fig. 9 for the 0.24 m diameter column. This implies that there is very good exchange between the liquid in the open and packed channels. From a reactor engineering standpoint this is good news because the liquid flowing in the packed channels is in intimate contact with the catalyst whereas the liquid in the open channels does not "see" the catalyst phase. However, because there is excellent interchange between the liquid phases present in the open channels and packed channels, the contacting efficiency of the liquid is not impaired by flow through the open channels.

The axial dispersion coefficient of the liquid phase $D_{ax,L}$ can be determined by fitting the measured response to

$$E(t/\tau) = \frac{1}{2\sqrt{\pi\alpha/\tau Pe}} \exp\left[-(1-t/\tau)^2 / (\pi\alpha/\tau Pe)\right] \quad (8)$$

where the Peclet number, Pe , and average liquid phase residence time τ are defined by

$$Pe \equiv \frac{U_L L}{\varepsilon_L D_{ax,L}} = \frac{v_L L}{D_{ax,L}}; \quad \tau \equiv \frac{L}{(U_L / \varepsilon_L)} \quad (9)$$

The values of the axial dispersion coefficient $D_{ax,L}$ are presented in Fig. 10 as a function of the liquid phase Reynolds number, defined in terms of the hydraulic

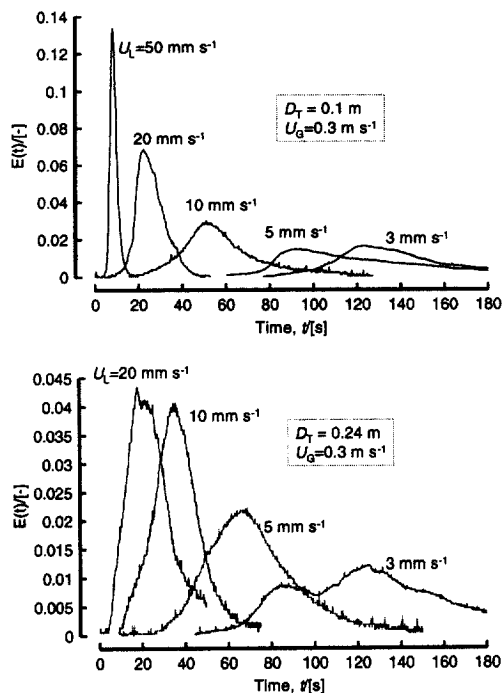


Figure 8. Liquid residence time distribution for the 0.1 and 0.24 m diameter columns measured at various superficial liquid velocities.

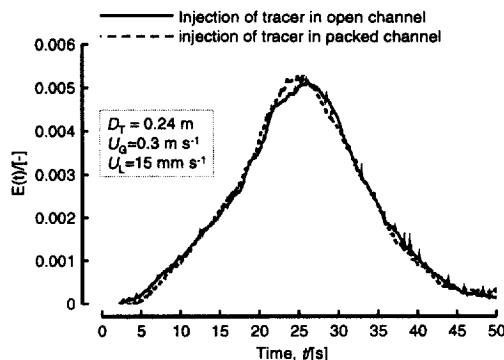


Figure 9. Liquid residence time distribution for the 0.24 m diameter column measured with two different tracer injection strategies: (a) tracer injection in the packed section and (b) tracer injection in the liquid in the open channels.

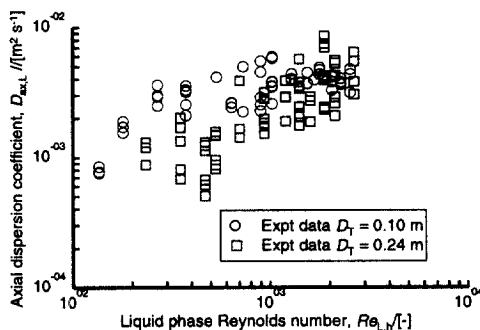


Figure 10. Liquid phase axial dispersion coefficient for structured packed columns.

diameter, $Re_{L,h}$. We note that the values of the axial dispersion coefficient $D_{ax,L}$ are practically independent of the column diameter and depend only on $Re_{L,h}$. The axial dispersion coefficients $D_{ax,L}$ for the structured packed columns are roughly about one order of magnitude higher than the corresponding values for trickle bed operation (Sie and Krishna, 1998). This is shown in Fig. 11 which compares the Bodenstein number, defined by

$$Bo \equiv \frac{v_L d_p}{D_{ax,L}} \quad (10)$$

for trickle beds and the catalytically structured packed column, operating in counter-current flow. The reason for the high dispersion coefficient in counter-current structured packed beds is the fact that the liquid flowing down the column enters both the open and packed channels; see Fig. 12. The liquid flowing through the packed channels sections has a much longer residence time than the liquid which flows through the open channels. The "bypassing" of the liquid through the open channels is the reason for the much larger dispersion coefficient measured for the structured packed columns. Such large-scale by-passing is not

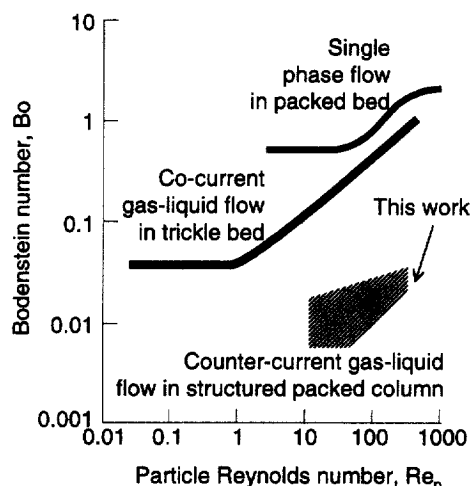


Figure 11. Comparison of Bodenstein number for cocurrent-downflow trickle beds, with counter-current flow in structured packed beds. The data for trickle beds (single phase and two-phase) has been taken from Sie and Krishna (1998).

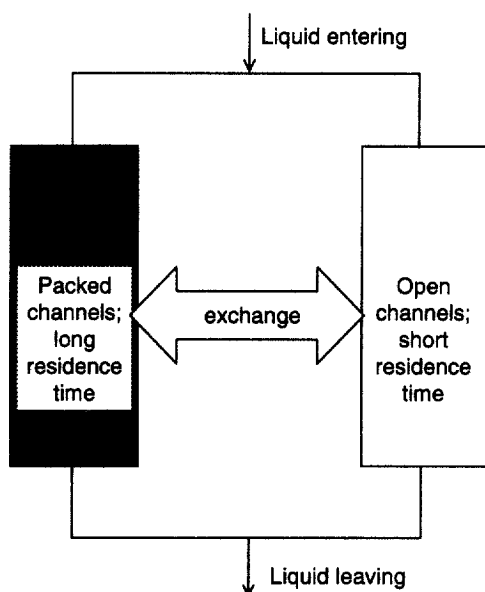


Figure 12. Schematic of liquid flow in structured packed column. The entering liquid flows both through the open and packed channels. There is excellent exchange between the liquid in the open and packed channels.

possible in conventional trickle bed operation. The "channelling" in cocurrent-downflow trickle bed operation takes place at the level of the particle diameter (which is of the order of 1-2 mm).

The high axial dispersion coefficients for the liquid phase in structured packed columns is not of great consequence for commercial columns with heights exceeding say 3 m; in such cases plug flow of the liquid phase is assured. However for short laboratory reactors shorter than say 0.5 m in height would suffer from backmixing of the liquid and this would need to be taken into account when interpreting reaction kinetics data (Bart and Landschützer, 1996).

OPERATING WINDOW OF A STRUCTURED PACKED COLUMN VERSUS TRICKLE BED

In order to compare the performance of the structured catalytically packed column with the conventional trickle bed, we also performed measurements for the pressure drop in a 0.07 m diameter trickle bed packed with 1.5 mm quadrulobe catalysts. At a superficial liquid velocity $U_L = 7$ mm/s, typical of industrial hydrotreating operations, the pressure drop per unit length of packing for the 0.07 m trickle bed (operating in co-current downflow) is compared with the performance of the structured catalytically packed columns in Fig. 13. The structured catalytically packed column has a pressure drop which is three orders of magnitude lower than that of the trickle bed, emphasizing its advantages for use in processes such as catalytic distillation, hydroconversion, etc.

Figure 14 compares the operating boundary for the trickle bed with the flooding boundary of the structured catalytically packed column of 0.1 m diameter. The operating window for trickling flow in a trickle bed reactor is relatively small. Outside this region the reactor will operate in the undesirable pulse or spray flow regime. The catalytically structured packed bed reactor can be operated at much higher superficial gas and liquid velocities, without flooding problems, than for conventional trickle bed operations.

CONCLUDING REMARKS

Counter-current operation of gas and liquid phases is important in many catalytic processes such as reactive distillation. As discussed by Krishna and Sie (1994) there are many significant advantages with counter-current operation for hydrotreating operations, which are classically carried out in co-current downflow trickle beds. The work described in this paper concerns the hydrodynamics and mixing characteristics of structured catalytically packed bed reactors, operating in counter-current flow of gas and liquid.

We have studied the pressure drop, liquid holdup and liquid phase residence time distribution of catalytically structured packed columns of 0.1 and 0.24 m diameter with counter-current flow of gas and liquid. The pressure drop in such structured columns is about three orders of magnitude lower than that of conventional

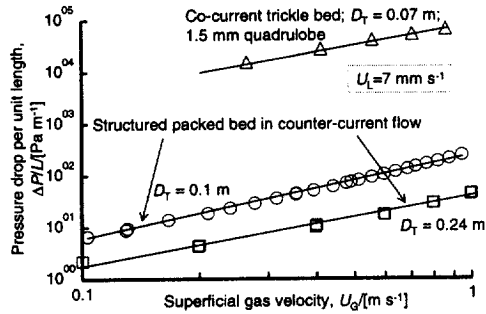


Figure 11. Comparison of pressure drops measured in a co-current trickle bed with that of structurally packed bed reactors in counter-current flow

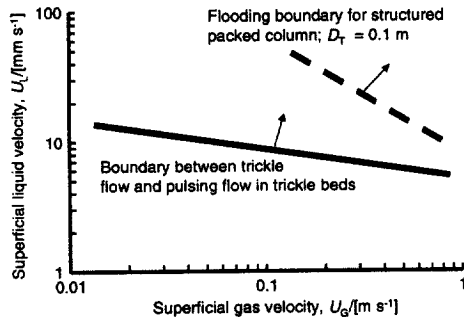


Figure 12. Comparison of operating boundary for a co-current trickle bed with flooding boundary for the structurally packed column of 0.1 m diameter.

trickle bed reactor operating in co-current flow. The liquid flows down the structured packed columns both within the packed channels and in the open channels, which is reserved for the gas phase. The interaction of gas and liquid in the open channels causes a substantial pressure drop. From measurements of liquid phase residence time distributions, we conclude that there is a very good exchange of liquid in the open channels and the packed channels. This is a desirable feature for applications in reactive distillation and hydrotreating.

NOTATION

| | |
|------------|---|
| A_{sp} | specific surface of "open" channels, m^{-1} |
| Bo | Bodenstein number, eq. (10), - |
| d_h | hydraulic diameter, m |
| d_p | particle diameter, m |
| $D_{ax,L}$ | axial dispersion coefficient, $m^2 s^{-1}$ |
| D_T | diameter of reactor, m |
| E | exit age distribution function, - |
| f | Fanning friction factor, - |
| Fr | Froude number, - |
| g | acceleration of gravity, $9.81 m s^{-2}$ |
| L | length of reactor, m |
| Pe | Péclet number, $Pe \equiv \frac{v_L L}{D_{ax,L}}$, - |
| Re | Reynolds number, - |

$Re_{L,h}$ Reynolds number based on hydraulic diameter,

$$Re_{L,h} \equiv \frac{v_L \rho_L d_h}{\eta_L}, -$$

Re_p particle Reynolds number, $Re_p \equiv \frac{v_L \rho_L d_p}{\eta_L}, -$

t time, s

U_G superficial velocity of gas phase, $m s^{-1}$

U_L superficial velocity of liquid phase, $m s^{-1}$

V volume, m^3

v_L interstitial liquid velocity within the packed channels, $m s^{-1}$

Greek letters

α angle of inclination, rad

ϵ volume fraction, -

ϵ_{OC} volume fraction of open channels, -

ϵ_{PC} volume fraction of packed channels, -

ρ density, $kg m^{-3}$

η dynamic viscosity, Pa s

σ surface tension, $N m^{-1}$

τ mean residence time, s

ΔP pressure drop, Pa

Subscripts

| | |
|-----|-----------------------|
| dry | dry |
| h | hydraulic |
| max | maximum |
| G | gas phase |
| L | liquid phase |
| OC | open channel |
| p | referring to particle |
| PC | packed channel |
| T | tower or column |

REFERENCES

Bart, H.-J. and Landschützer, H., (1996) Heterogene Reaktivdestillation mit axialer Rückvermischung, *Chem. Ing. Tech.*, **68**, 944-946 (1996)

Cho, S.Y., Lee, Y.Y. and Kim, S.J. (1995) A study of characteristics of a modern structured packing, *Korean J. of Chem. Eng.*, **12**, 313 – 319.

Van Gulijk, C. (1998) Using computational fluid dynamics to calculate transversal dispersion in a structured packed bed, *Computers in Chemical Engineering*, **22**, S767-S770.

Krishna, R. and Sie, S.T. (1994) Strategies for Multiphase Reactor Selection, *Chem.Engng Sci.*, **49**, 4029-4065

Sie, S.T. and Krishna, R. (1998) Process Development and Scale Up: III. Scale up and scale down of trickle bed processes, *Reviews in Chemical Engineering*, **14**, 203 – 252.

Xu, X., Zhao, Z. and Tian, S.-J. (1997) Study on catalytic distillation processes, Part III. Prediction of pressure drop and holdup in catalyst bed, *Trans.I.Chem.E. Part A*, **75**, 625 – 629.